Review

CellPress

Special Issue: Wiring and Rewiring in Signal Transduction

Ultrasensitivity part I: Michaelian responses and zero-order ultrasensitivity

James E. Ferrell Jr. and Sang Hoon Ha

Department of Chemical and Systems Biology, Stanford University School of Medicine, Stanford, CA 94305-5174, USA

Quantitative studies of signal transduction systems have shown that ultrasensitive responses – switch-like, sigmoidal input/output relationships – are commonplace in cell signaling. Ultrasensitivity is important for various complex signaling systems, including signaling cascades, bistable switches, and oscillators. In this first installment of a series on ultrasensitivity we survey the occurrence of ultrasensitive responses in signaling systems. We review why the simplest mass action systems exhibit Michaelian responses, and then move on to zero-order ultrasensitivity, a phenomenon that occurs when signaling proteins are operating near saturation. We also discuss the physiological relevance of zero-order ultrasensitivity to cellular regulation.

Cooperativity and the binding of oxygen to hemoglobin

The curve that relates hemoglobin oxygen binding to the partial pressure of oxygen is, famously, sigmoidal rather than hyperbolic. The sigmoidal shape is biologically significant; it means that hemoglobin can unload a greater fraction of its oxygen in the peripheral tissues than it otherwise could (Figure 1). Building upon the work of Hill [1], Adair [2], and Pauling [3], by the 1960s Monod, Wyman, and Changeux [4] and Koshland, Némethy, and Filmer [5] had proposed plausible alternative models to account for the sigmoidal curve. The models differ in a number of respects, but share several features. Both models make use of the fact that hemoglobin is a multi-subunit protein complex, and assume that allosteric regulation occurs both within its subunits and between subunits. In addition, both assume that there is cooperativity: that the binding of oxygen to the first sites promotes the binding of oxygen to the remaining sites. Cooperativity proved to be important not only for oxygen transport but also for many other processes, including signal transduction, where multimeric ion channels, receptor proteins, and transcription factors are now known to exhibit cooperativity and sigmoidal input–output relationships. Cooperativity is important and beautiful, but complicated, because it generally depends upon coordinated and precise interactions among many amino acids.

In 1981 Goldbeter and Koshland published a landmark paper showing that, in signal transduction pathways, a much simpler mechanism can yield sigmoidal response curves that resemble those of cooperative proteins. They called the phenomenon zero-order ultrasensitivity; 'zero-order' because it required that the signaling enzymes are operating close to saturation, and 'ultrasensitivity' because the sensitivity of the response, as defined in a particular way (discussed later), was higher than that seen if the enzymes were operating far from saturation [6].

Over the past decade it has become clear that ultrasensitive responses do occur in natural biological systems, and may in fact be commonplace in signal transduction (Table 1). In this series we review four basic classes of mechanism that can generate ultrasensitive responses, starting with zero-order ultrasensitivity and then moving on to multistep mechanisms, stoichiometric inhibitors, and positive feedback loops, as well as the experimental evidence that these mechanisms are relevant to cell signaling. We discuss several interesting variations and elaborations on these mechanisms that have emerged out of recent theoretical work. Finally, we look at how ultrasensitivity can be crucial in the generation of other emergent systems-level behaviors in more complex systems such as cascades, switches, and oscillators. In this way, ultrasensitive monocycles are

Glossary

Cooperativity: a characteristic of some multistep processes where completing some of the early steps makes a later step more favorable. Examples include the multistep binding of oxygen to hemoglobin and priming in multisite phosphorylation.

Hill function: an input–output relationship of the form $Output = \frac{Input^n}{K^n + Input^n}$, where n is the Hill exponent or Hill coefficient.

Mass action kinetics: a simple kinetic scheme where the rate of a reaction is directly proportional to the concentration of the substrate or substrates involved in the reaction. This contrasts with Michaelis–Menten kinetics or kinetic schemes involving Hill functions.

Michaelis–Menten kinetics: a model for the rate of an enzymatic reaction, premised on the assumption that the enzyme is small in concentration compared to its substrate, and that the concentration of the enzyme–substrate complex is unchanging with respect to time. In the Michaelis–Menten model the rate of an enzymatic reaction is given by $\frac{dProduct}{dt} = V_{\max}\frac{Substrate}{K_m + Subtrate}$.

Ultrasensitivity: a property of steady-state input–output relationships that makes them switch-like in character. Goldbeter and Koshland defined input–output relationships to be ultrasensitive if it took less than an 81-fold change in input stimulus to drive the output from 10% to 90% of maximum.

Zero-order: a zero-order chemical or biochemical reaction is one where the rate of the reaction is independent of the substrate concentration. Enzyme reactions approach zero-order when the enzyme is saturated with substrate.

Corresponding author: Ferrell, J.E. Jr. (james.ferrell@stanford.edu).

0968-0004/
 http://dx.doi.org/10.1016/j.tibs.2014.08.003

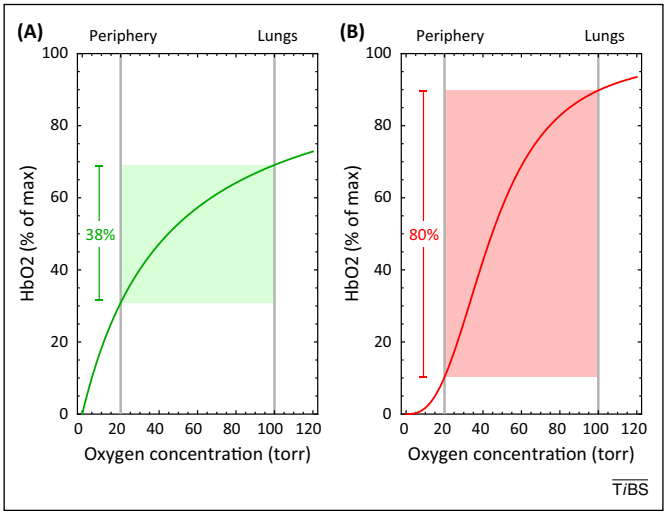

Figure 1. The binding of oxygen to hemoglobin. If the binding curve were hyperbolic **(A)**, at best 38% of its oxygen could be delivered to the peripheral tissues. However, in reality the binding curve is sigmoidal with an apparent Hill coefficient of 2.7 **(B)**. A sigmoidal curve with this Hill coefficient could allow hemoglobin to deliver as much as 80% of its oxygen.

important elements in the generation of sophisticated biochemical behaviors.

Further perspectives on ultrasensitivity can be found in several recent papers [7–9] as well as in the classic papers of Goldbeter and Koshland [6,10–12]. We begin with an examination of Michaelian responses and zero-order ultrasensitivity.

Hyperbolic or Michaelian steady-state responses

Before examining how ultrasensitive responses are generated it is helpful to thoroughly understand the responses of simple systems that are not ultrasensitive. Suppose that we have a signaling protein X that can be activated by phosphorylation and inactivated by dephosphorylation (Figure 2A). If we assume mass-action kinetics (see Glossary), it follows (Box 1) that the steady-state input–output relationship for the system is given by Equation 1, where *Input* represents the concentration of the kinase driving the reaction, *Output* is the fraction of X in the phosphorylated form, and K is the $EC50$ (effective concentration 50%) for the system; that is, level of *Input* where half of the X is phosphorylated.

$$Output = \frac{Input}{K + Input} \quad [1]$$

This relationship is plotted in Figure 2. Because the functional form of the equation is the same as that of the Michaelis–Menten equation, this type of response is sometimes referred to as Michaelian [12]. Note though that the Michaelis–Menten equation relates substrate concentrations to the initial rates of enzyme reactions, and not kinase concentrations to the steady-state levels of substrate phosphorylation as we have here. Also note that here we have assumed that the enzyme reactions are described by the law of mass action, and not by Michaelis–Menten kinetics. This fact is perhaps worth repeating because the terminology can be confusing: a Michaelian steady-state response is not generated by systems where enzyme activities are described the Michaelis–Menten equation. It is generated by systems where the law of mass action applies.

Michaelian responses are also obtained when an output is generated by ligand binding (e.g., activation of monomeric receptors by monomeric hormones), regulated

Table 1. Some examples of ultrasensitivity in signal transduction

Stimulus	Response	Effective Hill exponent	Experimental system	Refs
Acetylcholine	Nicotinic cholinergic receptor conductance	1.3	Chicken neuronal homomeric α7 receptors	[23]
Delta (in trans only)	Notch production	1.7	CHO cells	[24]
Mos	MEK1	1.7	*Xenopus laevis* oocyte extracts	[25]
Phosphorylase kinase/phosphatase	Glycogen phosphorylase	2	Reconstituted mammalian muscle enzymes	[21]
RsbQP	σ^B	2.1	*Bacillus subtilis*	[26]
AICAR	AMPK	2.5	Rat INS-1 cells	[27]
Ca^{2+}	Calmodulin-dependent cAMP phosphodiesterase	2.7[a]	Purified beef heart proteins	[28]
IP_3	Calcium release	3	Permeabilized rat basophilic leukemia cells	[29]
Cdk1	Wee1A	3.5	*Xenopus laevis* egg extracts	[30]
Anisomycin	Jnk	3–10	HeLa, HEK293, and Jurkat cells	[31]
Sorbitol	Jnk	4–9	HeLa, HEK293, and Jurkat cells	[31]
Mos	Erk2	5	*Xenopus laevis* oocytes	[25]
Cln2	Cln2 synthesis	5	*S. cerevisiae*	[32]
KinA	σ^E and σ^F	10	*Bacillus subtilis*	[33]
CheY-P	Flagellar motor output	~10–20	*Escherichia coli*	[34–36]
Cdk1	Cdc25C	11	*Xenopus laevis* egg extracts	[37]
Delta (cis and trans)	Notch production	12	CHO cells	[24]
Cdk1	APC/C^{Cdc20}	≥17	*Xenopus laevis* egg extracts and embryos	[38,39]
Yan	ERK	Not determined	*Drosophila embryos*	[22]

[a]Our estimate based on the data in Figure 3 from [28].

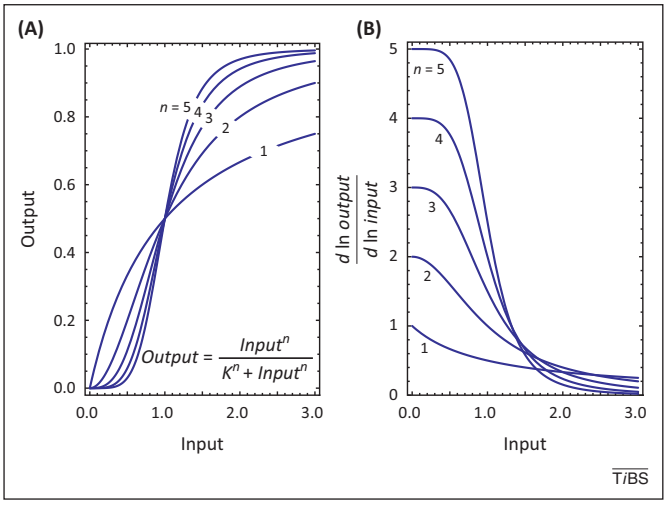

Figure 2. Ultrasensitivity and the Hill function. **(A)** Input–output relationships for Hill functions with exponents of 1, 2, 3, 4, and 5. When $n = 1$ the response is the same as a Michaelian response. When $n > 1$, the response is ultrasensitive, and the greater the value of n, the more switch-like the response. **(B)** Local sensitivities, as measured by the function $\frac{dlnOutput}{dlnInput}$, for Hill curves with exponents of 1, 2, 3, 4, and 5. Note that the local sensitivity is the same as the polynomial order of the curve, and at low values of *Input* the sensitivity approaches n.

synthesis (e.g., transcription, translation, or second messenger synthesis), or translocation (e.g., the recruitment of Raf or Akt to the plasma membrane) provided that the input regulates one step in the process and simple mass-action kinetics apply.

Defining sensitivity and ultrasensitivity

In common parlance, the terms 'sensitive' and 'sensitivity' usually refer to how much input is needed to achieve a particular level of output. An assay that detects 1 ng of flu virus is more sensitive than one that detects 1 μg, and one might call an assay that detects a remarkably low amount of virus ultrasensitive. If one looks at recent scientific publications, sensitivity and ultrasensitivity are sometimes used in this sense, particularly in assay development (e.g., [13]). A common measure of this type of sensitivity is the *EC*50, which is the amount of input required to achieve a half-maximal output. The lower the *EC*50, the higher the sensitivity.

Goldbeter and Koshland used the term sensitivity in a different sense, however, to denote the relationship between a change in input and a change in output. To make sensitivity independent of the units used, they expressed the changes in input and output as fold changes: $\frac{\Delta Input}{Input}$ *and* $\frac{\Delta Output}{Output}$, with the sensitivity being the ratio of the latter to the former. One can define sensitivity locally (S_{local}) by assuming that the change in *Input* is infinitesimal (Equation 2).

$$S_{local} = \lim_{\Delta Input \to 0} \frac{\Delta Output}{Output} \Big/ \frac{\Delta Input}{Input} = \frac{dOutput}{dInput} \cdot \frac{Input}{Output} = \frac{d\ln Output}{d\ln Input} \quad [2]$$

The higher the value of S_{local}, the higher the sensitivity. Note that S_{local} is the slope of a log–log plot of *Input* vs *Output*, which makes it the polynomial order of the response. For a Michaelian response, where the response approaches first-order for small stimuli and zero-order for large stimuli, S_{local} is approximately 1 for small inputs, falls to 0.5 when the input equals the *EC*50, and approaches 0 for large inputs (Figure 2). For a Hill function, S_{local} is approximately equal to n for small inputs and approaches 0 for large inputs (Figure 2). Local sensitivity will be useful when we discuss signaling cascades later in this article.

Alternatively, one can calculate an overall, global value for the sensitivity of an input–output curve. Typically this is taken as the *EC*90:*EC*10 ratio. For a Michaelian response the ratio is always 81, and Goldbeter and Koshland therefore defined an ultrasensitive response as any response with an *EC*90:*EC*10 ratio smaller than 81 [6,10,12].

An ultrasensitive response is often (though not always) sigmoidal – flat at high and low inputs and steep in between – and often the curve is well-approximated by the Hill equation. This fact suggests another way of globally quantifying sensitivity, from the effective Hill exponent, which is defined as the Hill exponent n for a Hill curve (Equation 3 and Figure 2) that has the same *EC*90:*EC*10 ratio as the response curve in question.

$$Output = \frac{Input^n}{K^n + Input^n} \quad [3]$$

The effective Hill exponent is related to the *EC*90:*EC*10 ratio by Equation 4 [14]:

$$n = \frac{\mathrm{Log}[81]}{\mathrm{Log}[EC90/EC10]} \quad [4]$$

There are problems with this definition if the basal level of response is high, or if the response is not well-approximated by the Hill equation (e.g., if it is a bell-shaped response). In these cases, a more general, but also more complicated, integrated response coefficient can be used to characterize the global ultrasensitivity [9]. However, for present purposes, the effective Hill exponent is an

Box 1. Michaelian responses

Here we derive the steady-state response of a simple phosphorylation–dephosphorylation system (see Figure 2A in main text). If we assume mass action kinetics, the net rate of phosphorylation is:

$$\frac{dXP}{dt} = k_1 kinase(X_{tot} - XP) - k_{-1}\, p'ase \cdot XP \quad [I]$$

where k_1 is the rate constant for phosphorylation, k_{-1} is the rate constant for dephosphorylation, and *p'ase* is the concentration of the phosphatase. We do not need to write an equation for the other time-dependent species, *X*; because producing one molecule of *XP* takes away one molecule of *X*, this single rate equation describes the dynamics of both *X* and *XP*. This ordinary differential equation can be solved: *XP* exponentially approaches its steady-state level with a half-time of $k_1 kinase + k_{-1} p'ase$. However, for present purposes, we need only an expression for the steady-state level of *XP*, which can be obtained by solving an algebraic equation. At steady state the net rate of phosphorylation is zero; it follows that:

$$Output = \frac{Input}{K + Input} \quad [II]$$

We have taken the input to be the concentration of the kinase, the output to be the fraction of *X* that is phosphorylated. The constant represents the *EC*50 for the system because when *Input* = *K*, $Output = \frac{K}{2K} = 0.5$.

Box 2. Zero-order ultrasensitivity

For a phosphorylation–dephosphorylation reaction with saturable enzymatic reactions rather than mass action kinetics, the situation becomes more complicated. Assuming that the total concentration of the substrate X is the sum of the concentrations of X and XP (i.e., the concentrations of the $kinase \cdot X$ and $p'ase \cdot XP$ complexes are negligible), the system can be described by a single rate equation:

$$\frac{dXP}{dt} = k_1 kinase \frac{X_{tot} - XP}{K_{m1} + X_{tot} - XP} - k_{-1}\, p'ase \frac{XP}{K_{m2} + XP} \quad [I]$$

Here K_{m1} and K_{m2} are the Michaelis constants for the kinase and phosphatase, respectively. At steady state:

$$k_1 kinase \frac{X_{tot} - XP_{ss}}{K_{m1} + X_{tot} - XP_{ss}} - k_{-1}\, p'ase \frac{XP_{ss}}{K_{m2} + XP_{ss}} = 0 \quad [II]$$

Equation II can be solved for XP_{ss}, the steady-state concentration of XP, analytically, yielding the Goldbeter–Koshland equation:

$$XP_{ss} = \frac{k_1 X_{tot} kinase - k_1 K_{m2} kinase - k_{-1} K_{m1}\, p'ase - k_{-1} X_{tot}\, p'ase + \sqrt{k_{-1}(K_{m1} + X_{tot})^2\, p'ase + k_1(K_{m2} + X_{tot}) + 4k_1 K_{m2} X_{tot} kinase(k_1 kinase - k_{-1}\, p'ase)}}{2k_1 kinase - 2k_{-1}\, p'ase} \quad [III]$$

Similarly, if we assume that the phosphatase reaction is saturable but the kinase reaction is described by mass action kinetics, it follows that:

$$XP_{ss} = \frac{-K_{m2} kinase - p'ase + X_{tot} kinase + \sqrt{4kinase^2 K_{m2} X_{tot} + (-K_{m2} kinase - p'ase + X_{tot} kinase)^2}}{2kinase} \quad [IV]$$

And if we assume that the kinase reaction is saturable and the phosphatase is described by mass action kinetics, it follows that:

$$XP_{ss} = \frac{k_1 kinase + k_{-1}\, p'ase(K_{m1} + X_{tot}) + \sqrt{-4k_1 k_{-1} kinase \cdot p'ase \cdot X_{tot} + (k_1 kinase + k_{-1}\, p'ase(K_{m1} + X_{tot}))^2}}{2k_{-1}\, p'ase} \quad [V]$$

Note that Equation III can be simplified slightly by defining $V_1 = k_1 kinase$, $V_{-1} = k_{-1} p'ase$, $\hat{K}_{m1} = K_{m1}/X_{tot}$, and $\hat{K}_{m2} = K_{m2}/X_{tot}$ and dividing through by X_{tot}:

$$\frac{XP_{ss}}{X_{tot}} = \frac{\frac{V_1}{V_{-1}}\left(1 - \hat{K}_{m2}\right) - \hat{K}_{m1} - 1 + \sqrt{4\hat{K}_{m2}\frac{V_1}{V_{-1}}\left(\frac{V_1}{V_{-1}} - 1\right) + \left(\frac{V_1}{V_{-1}}\left(\hat{K}_{m2} - 1\right) + \hat{K}_{m1} + 1\right)^2}}{2\left(\frac{V_1}{V_{-1}} - 1\right)} \quad [VI]$$

This is the usual form of the Goldbeter–Koshland equation.

adequate way of quantifying sensitivity and ultrasensitivity, and we will use this way of quantifying ultrasensitivity in most of the discussion of this article.

Zero-order ultrasensitivity

Suppose that we have a phosphorylation–dephosphorylation monocycle, but now instead of having enzymes whose activities are given by the law of mass action, the enzymes are saturable and their activities are given by the Michaelis–Menten equation. As shown in Box 2, the steady-state response of the system is now described by the formidable Goldbeter–Koshland equation (Equation III in Box 2). It is not easy to intuit much from merely looking at this complicated equation, but if one plugs in values for the parameters such that both the phosphorylation and dephosphorylation reactions are running close to saturation, and then plots the fraction of the substrate X that is phosphorylated (XP/X_{tot}) as a function of *kinase*, the result is indeed a highly ultrasensitive, sigmoidal curve (Figure 3D). A good way to understand why the curve is shaped this way is through a simple graphical method, the rate-balance plot.

Rate-balance plots

The basic idea of the rate-balance plot is to isolate the terms in the rate equation that increase the amount of XP, which contribute to the phosphorylation rate, and the terms that decrease the amount of XP, which contribute to the dephosphorylation rate [15–18]. The phosphorylation rate and dephosphorylation rate curves are then both plotted as a function of XP on one set of axes. Wherever the curves cross, the rates of phosphorylation and dephosphorylation are equal and the system is in steady state. One can then examine how the steady-state level of XP depends upon, for example, the concentration of kinase present. Following Gomez-Uribe *et al.* [19], we will consider four regimes of operation of the phosphorylation–dephosphorylation cycle: saturating neither reaction, both reactions, or one or the other.

If we assume mass action kinetics for both the phosphorylation and dephosphorylation reactions (Figure 3A), the rate curves are straight lines whose slopes are determined by the rate constants and enzyme concentrations. By plotting the values of XP/X_{tot} at the intersection points as a function of the assumed kinase concentration, one can build up an input–output curve (Figure 3A, right) which, of course, agrees with Equation 1. Note that the first increment of input (*kinase*) produces a reasonable increment of output, and then each successive increment produces less (Figure 3A, left). Thus, the rate-balance analysis provides an intuitive feel for why mass action kinetics produces a response with a 'diminishing returns' quality.

Next, we assume that the phosphatase is operating near saturation, with a K_m value 100-fold lower than the total concentration of the substrate X (Figure 3B). The phosphorylation rate curves are unchanged, but the dephosphorylation rate curve becomes a hyperbola, with the dephosphorylation rate being half-maximal when XP = 0.01 units. Now the first increments of input produce very little output until the phosphorylation rate curve reaches the knee of the dephosphorylation rate curve (Figure 3B). Saturation of the phosphatase builds a threshold into the

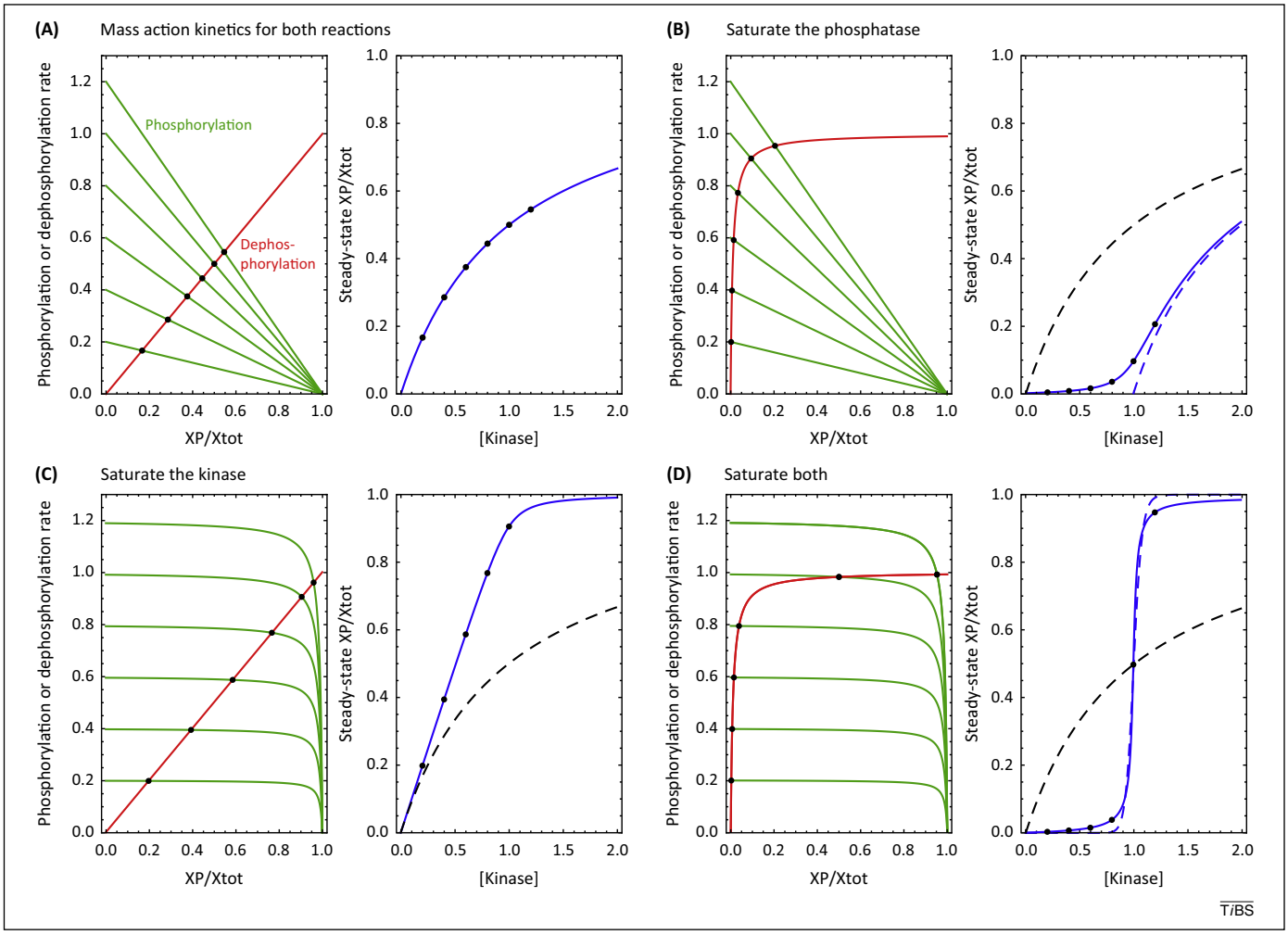

Figure 3. Michaelian responses and zero-order ultrasensitivity: rate-balance analysis. **(A)** Rate balance analysis assuming mass action kinetics, which yield a Michaelian response. **(B–D)** Rate balance analysis assuming that one or both of the reactions is running close to saturation. In each panel, the left-hand plot shows the rate curves, with the phosphorylation rates being shown in green and the dephosphorylation rates shown in red. The intersection points (filled black circles) correspond to steady states. The right-hand plots show the input ([*kinase*]) vs output (the fraction of X_{tot} phosphorylated at steady state) relationships in unbroken blue, as described by Equations III–V in Box 2. The filled black circles are the same steady states shown in the left-hand plots. The broken black curves in panels B–D show Michaelian input–output relationships, for comparison, and the broken blue curve in panel B shows a Michaelian input–output curve shifted one concentration unit to the right. The assumed kinetic parameters were: $k_1 = k_{-1} = X_{tot} = p'ase = 1$; $K_{m1} = K_{m2} = 0.01$; and *kinase* = 0.2, 0.4, 0.6, 0.8, 1.0, or 1.2. The effective Hill coefficients for the blue curves are 1, 1.18, 2, and 26.1, respectively. The broken blue line in panel D shows a Hill function with a Hill exponent of 26.1 for comparison. Similar input–output curves can be found in [19].

response, and as the K_m values for the phosphatase approaches zero, the input–output curve approaches a Michaelian response that has been shifted to the right by one concentration unit (Figure 3B, right). By Goldbeter and Koshland's definition, the response is slightly ultrasensitive; as the saturation increases, the ratio $\frac{EC90}{EC10}$ approaches 41, which is less than 81, and the effective Hill exponent is 1.18. Gomez-Uribe and coworkers dubbed this a threshold-hyperbolic response [19].

By contrast, if the kinase is operating near saturation but the phosphatase is not (Figure 3C), there is no threshold in the steady-state response (Figure 3C, right). Instead, the response approaches its maximal value more abruptly than a Michaelian response does (Figure 3C, right). This is because when the phosphorylation rate curves are virtually flat (Figure 3C, left) the kinase activity does not fall off much as the output (XP/Xtot) increases. The response curve approaches a straight line that does not bend over until the response is nearly maximal. By Goldbeter and Koshland's definition, this curve is ultrasensitive because for a straight line the $EC90$:$EC10$ ratio is 9 and the effective Hill exponent (Equation 3) is 2. However, nowhere on the curve is the local sensitivity (the polynomial order) greater than 1, and for clarity it is probably better to call this a linear response rather than an ultrasensitive one.

Note that in principle linear responses could be extremely useful in signal transduction [19]. In the mating pheromone pathway in *Saccharomyces cerevisiae*, the response of the terminal protein kinase in the response pathway (Fus3) is, indeed, a nearly linear function of the pheromone concentration [20], and the mechanisms underpinning this linearity are not understood. Saturated signal transducers could help to provide this linearity, as could some of the mechanisms that will be discussed later in this series (e.g., multisite phosphorylation with 'OR gate' logic and stoichiometric inhibitors).

Finally, if both the kinase and phosphatase are assumed to be close to saturation, the response shows both a threshold and an abrupt leveling off at maximal response (Figure 3D). The result is a steeply sigmoidal input–output

relationship (Figure 3D, right). The curve is similar (but not identical) in shape to a Hill function (Figure 3D, right, unbroken vs broken blue curves), and the effective Hill exponent for the degree of saturation assumed in Figure 3D is huge: 26.1. Thus, saturation of the kinase and phosphatase synergize to produce switch-like responses.

Competition in zero-order monocycles

So far we have assumed that only two species contribute significantly to the total pool of the substrate X_{tot}: the phosphorylated form *XP* and the dephosphorylated form *X*. However, we have also assumed that the kinase and phosphatase are operating close to saturation, which means that a large proportion of the kinase molecules are bound to *X* and the phosphatase to *XP*. These complexes will still be negligible compared to *X* and *XP* if the concentrations of the kinase and phosphatase are small compared to the concentration of the substrate. However, in signaling cascades, kinases, phosphatases, and their substrates are sometimes comparable in concentration. What would the steady-state response of a phosphorylation–dephosphorylation monocycle be if the assumption that the kinase and phosphatase are low in concentration were relaxed?

This situation was considered by Goldbeter and Koshland in their original paper [6]. The algebra becomes more complicated; there are now four rate equations for four time-dependent species (for *X, XP, X·kinase*, and *XP·p'ase*) and a conservation equation (X_{tot}=*X*+*XP*+*X·kinase*+*XP·p'ase*). It is no longer possible to carry out a simple one-variable rate-balance analysis or even an analytical solution, but solutions can be obtained numerically.

The results are shown in Figure 4. When the phosphatase is assumed to be 1/100 the concentration of its substrate, there is very little difference between the exact response curve and the curve given by the Goldbeter–Koshland equation (Figure 4A). When the phosphatase reaches 1/10 the substrate concentration, the response is still highly ultrasensitive, but the maximal response is lower because at high inputs 20% of the substrate is tied up in complexes (10% with the kinase and 10% with the phosphatase) (Figure 4B). And when the phosphatase is equal in concentration to the substrate, the maximal steady-state concentration of *XP* is very small (Figure 4C), with almost all of the substrate being present in complexes, and the sigmoidal character of the response is minimal (Figure 4, inset). Thus, zero-order ultrasensitivity is best generated when the converting enzymes are operating close to saturation and they are much lower in concentration than their substrate.

Physiological relevance of zero-order ultrasensitivity

Whereas the development of the theory of cooperativity was driven by experiment, most especially by the sigmoidal oxygen-binding curve of hemoglobin, this was not the case for zero-order ultrasensitivity. There was not some particular experimental mystery that zero-order ultrasensitivity was attempting to explain. The theory came first, and it then motivated and guided subsequent experimental studies.

The first experimental test of zero-order ultrasensitivity came in studies of isocitrate dehydrogenase (IDH) phosphorylation in a reconstituted system [15]. At concentrations of IDH above the K_m values for its phosphorylation and dephosphorylation, but still below that estimated to be present *in vivo*, a sigmoidal dose-response curve was obtained with a Hill coefficient of ~2 [15]. Zero-order ultrasensitivity was also demonstrated for the phosphorylation of glycogen phosphorylase *in vitro* [21] (Figure 5), and again the concentration of phosphorylase *in vivo* is thought to be high enough to make the *in vitro* results physiologically relevant. Finally, the response of the transcription factor Yan to the activation of the ERK MAP kinase in *Drosophila* ectodermal patterning has been shown to be ultrasensitive, and zero-order ultrasensitivity as a possible mechanism for this ultrasensitivity fits well

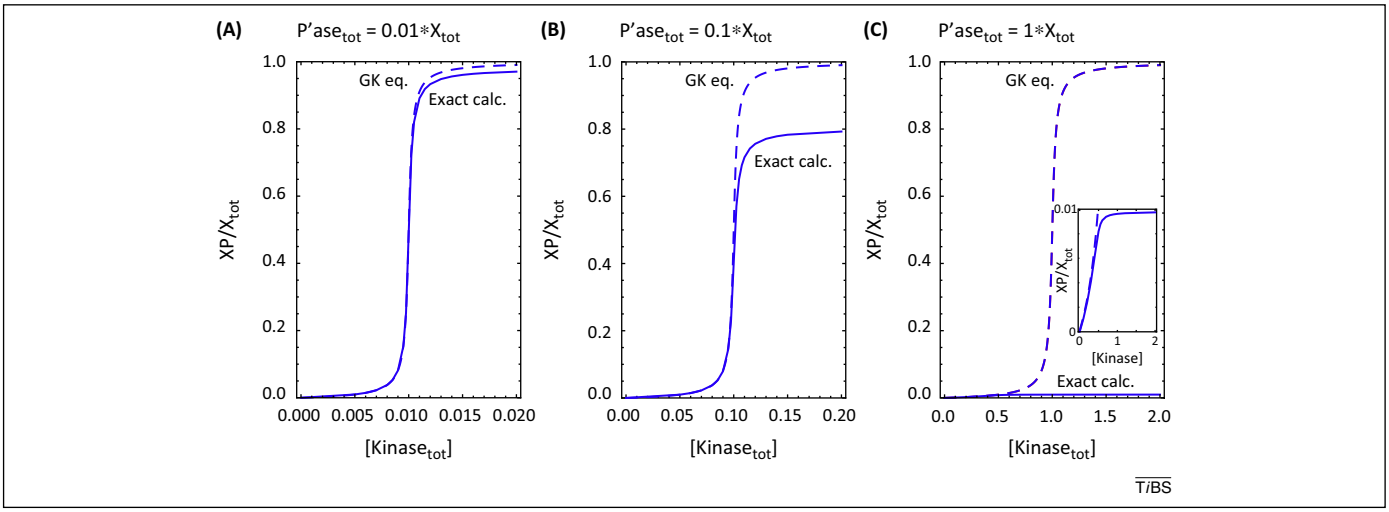

Figure 4. Zero-order ultrasensitivity requires that the converting enzymes be saturated and small in concentration compared to the substrate. **(A–C)** Goldbeter–Koshland response curves (GK eq., broken blue curves) compared with exactly-calculated response curves (Exact calc., unbroken blue curves), assuming various ratios of the converting enzymes to the substrate. In each case we assumed that the association (*a*), dissociation (*d*), and catalytic (*k*) rate constants for both phosphorylation and dephosphorylation were *a* = 200, *d* = 1 and *k* = 1. Thus, in each case the K_m values for both the phosphorylation and dephosphorylation reactions were 0.01 such that the total substrate concentration was 100-fold higher than the K_m values (i.e., both converting enzymes were operating close to saturation). The inset in panel C shows that at low total kinase concentrations, the two curves are similar.

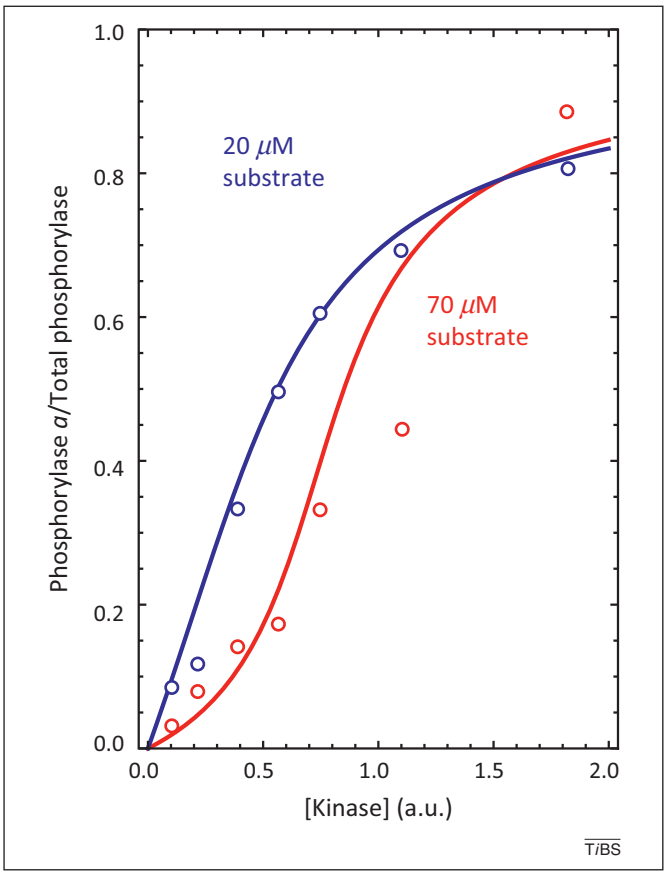

Figure 5. Zero-order ultrasensitivity in a reconstituted phosphorylase phosphorylation system. The fitted curves are from the Goldbeter–Koshland equation based on the measured K_m values, and the effective Hill coefficients were 1.35 (blue curve) and 2.35 (red curve). Adapted from [21].

with the observed insensitivity of patterning to Yan overexpression [22].

However, there are several examples of huge Hill coefficients, including some of those seen near the bottom of Table 1, that appear not to be due to zero-order ultrasensitivity alone. This raises the question of what other mechanisms can contribute to ultrasensitive responses. We will examine three such mechanisms, multisite phosphorylation, stoichiometric inhibitors, and positive feedback loops, in the next installment of this series.

Acknowledgments

This article is based on a talk given in Brussels in September 2012 in honor of Prof. Albert Goldbeter, and is respectfully dedicated to this theoretical biology pioneer. We thank Alisa Moskaleva and the rest of the laboratory of J.E.F. for helpful comments and discussions. This work was supported by grants from the National Institutes of Health (GM046383 and GM107615).

References

1 Hill, A.V. (1910) The possible effects of the aggregation of the molecules of haemoglobin on its dissociation curves. *J. Physiol.* 40, iv–vii Proceedings
2 Adair, G.S. (1925) The hemoglobin system. VI. The oxygen dissociation curve of hemoglobin. *J. Biol. Chem.* 63, 529–545
3 Pauling, L. (1935) The oxygen equilibrium of hemoglobin and its structural interpretation. *Proc. Natl. Acad. Sci. U.S.A.* 21, 186–191
4 Monod, J. *et al.* (1965) On the nature of allosteric transitions: a plausible model. *J. Mol. Biol.* 12, 88–118
5 Koshland, D.E., Jr *et al.* (1966) Comparison of experimental binding data and theoretical models in proteins containing subunits. *Biochemistry* 5, 365–385
6 Goldbeter, A. and Koshland, D.E., Jr (1981) An amplified sensitivity arising from covalent modification in biological systems. *PNAS* 78, 6840–6844
7 Salazar, C. and Hofer, T. (2006) Competition effects shape the response sensitivity and kinetics of phosphorylation cycles in cell signaling. *Ann. N. Y. Acad. Sci.* 1091, 517–530
8 Salazar, C. and Hofer, T. (2006) Kinetic models of phosphorylation cycles: a systematic approach using the rapid-equilibrium approximation for protein-protein interactions. *Biosystems* 83, 195–206
9 Legewie, S. *et al.* (2005) Quantitative analysis of ultrasensitive responses. *FEBS J.* 272, 4071–4079
10 Goldbeter, A. and Koshland, D.E., Jr (1982) Sensitivity amplification in biochemical systems. *Q. Rev. Biophys.* 15, 555–591
11 Goldbeter, A. and Koshland, D.E., Jr (1984) Ultrasensitivity in biochemical systems controlled by covalent modification. Interplay between zero-order and multistep effects. *J. Biol. Chem.* 259, 14441–14447
12 Koshland, D.E., Jr *et al.* (1982) Amplification and adaptation in regulatory and sensory systems. *Science* 217, 220–225
13 Li, Y. *et al.* (2013) Highly sensitive fluorescent immunosensor for detection of influenza virus based on Ag autocatalysis. *Biosens. Bioelectron.* 54C, 358–364
14 Taketa, K. and Pogell, B.M. (1965) Allosteric inhibition of rat liver fructose 1,6-diphosphatase by adenosine 5′-monophosphate. *J. Biol. Chem.* 240, 651–662
15 LaPorte, D.C. and Koshland, D.E., Jr (1983) Phosphorylation of isocitrate dehydrogenase as a demonstration of enhanced sensitivity in covalent regulation. *Nature* 305, 286–290
16 Ferrell, J.E., Jr (1996) Tripping the switch fantastic: how a protein kinase cascade can convert graded inputs into switch-like outputs. *Trends Biochem. Sci.* 21, 460–466
17 Thron, C.D. (1996) A model for a bistable biochemical trigger of mitosis. *Biophys. Chem.* 57, 239–251
18 Ferrell, J.E., Jr and Xiong, W. (2001) Bistability in cell signaling: how to make continuous processes discontinuous, and reversible processes irreversible. *Chaos* 11, 227–236
19 Gomez-Uribe, C. *et al.* (2007) Operating regimes of signaling cycles: statics, dynamics, and noise filtering. *PLoS Comput. Biol.* 3, e246
20 Yu, R.C. *et al.* (2008) Negative feedback that improves information transmission in yeast signalling. *Nature* 456, 755–761
21 Meinke, M.H. *et al.* (1986) Zero-order ultrasensitivity in the regulation of glycogen phosphorylase. *Proc. Natl. Acad. Sci. U.S.A* 83, 2865–2868
22 Melen, G.J. *et al.* (2005) Threshold responses to morphogen gradients by zero-order ultrasensitivity. *Mol. Syst. Biol.* 1, 2005.0028
23 Galzi, J.L. *et al.* (1996) The multiple phenotypes of allosteric receptor mutants. *Proc. Natl. Acad. Sci. U.S.A* 93, 1853–1858
24 Sprinzak, D. *et al.* (2010) Cis-interactions between Notch and Delta generate mutually exclusive signalling states. *Nature* 465, 86–90
25 Huang, C-Y.F. and Ferrell, J.E., Jr (1996) Ultrasensitivity in the mitogen-activated protein kinase cascade. *PNAS* 93, 10078–10083
26 Locke, J.C. *et al.* (2011) Stochastic pulse regulation in bacterial stress response. *Science* 334, 366–369
27 Hardie, D.G. *et al.* (1999) AMP-activated protein kinase: an ultrasensitive system for monitoring cellular energy charge. *Biochem. J.* 338 (Pt 3), 717–722
28 Teo, T.S. and Wang, J.H. (1973) Mechanism of activation of a cyclic adenosine 3′:5′-monophosphate phosphodiesterase from bovine heart by calcium ions. Identification of the protein activator as a Ca^{2+} binding protein. *J. Biol. Chem.* 248, 5950–5955
29 Meyer, T. *et al.* (1988) Highly cooperative opening of calcium channels by inositol 1,4,5-trisphosphate. *Science* 240, 653–656
30 Kim, S.Y. and Ferrell, J.E., Jr (2007) Substrate competition as a source of ultrasensitivity in the inactivation of Wee1. *Cell* 128, 1133–1145
31 Bagowski, C.P. *et al.* (2003) The JNK cascade as a biochemical switch in mammalian cells. Ultrasensitive and all-or-none responses. *Curr. Biol.* 13, 315–320
32 Charvin, G. *et al.* (2010) Origin of irreversibility of cell cycle start in budding yeast. *PLoS Biol.* 8, e1000284

33 Narula, J. *et al.* (2012) Ultrasensitivity of the *Bacillus subtilis* sporulation decision. *Proc. Natl. Acad. Sci. U.S.A* 109, E3513–E3522
34 Yuan, J. and Berg, H.C. (2013) Ultrasensitivity of an adaptive bacterial motor. *J. Mol. Biol.* 425, 1760–1764
35 Yuan, J. *et al.* (2012) Adaptation at the output of the chemotaxis signalling pathway. *Nature* 484, 233–236
36 Cluzel, P. *et al.* (2000) An ultrasensitive bacterial motor revealed by monitoring signaling proteins in single cells. *Science* 287, 1652–1655
37 Trunnell, N.B. *et al.* (2011) Ultrasensitivity in the regulation of Cdc25C by Cdk1. *Mol. Cell* 41, 263–274
38 Yang, Q. and Ferrell, J.E., Jr (2013) The Cdk1–APC/C cell cycle oscillator circuit functions as a time-delayed, ultrasensitive switch. *Nat. Cell Biol.* 15, 519–525
39 Tsai, T.Y. *et al.* (2014) Changes in oscillatory dynamics in the cell cycle of early *Xenopus laevis* embryos. *PLoS Biol.* 12, e1001788